NASA TECHNICAL MEMORANDUM

NASA TM X-2022

c. 1

NASA TM X-2022

HYDROGEN CAVITATION PERFORMANCE OF 80.6° HELICAL INDUCER WITH BLUNT LEADING EDGES

by Phillip R. Meng and Royce D. Moore

Lewis Research Center
Cleveland, Ohio 44135

NATIONAL AERONAUTICS AND SPACE ADMINISTRATION • WASHINGTON, D. C. • JULY 1970

1. Report No. NASA TM X-2022	2. Government Accession No.	3. Recipient's Catalog No.
4. Title and Subtitle HYDROGEN CAVITATION PERFORMANCE OF 80.6° HELICAL INDUCER WITH BLUNT LEADING EDGES		5. Report Date July 1970 6. Performing Organization Code
7. Author(s) Phillip R. Meng and Royce D. Moore		8. Performing Organization Report No. E-5495
9. Performing Organization Name and Address Lewis Research Center National Aeronautics and Space Administration Cleveland, Ohio 44135		10. Work Unit No. 128-31 11. Contract or Grant No. 13. Type of Report and Period Covered
12. Sponsoring Agency Name and Address National Aeronautics and Space Administration Washington, D.C. 20546		Technical Memorandum 14. Sponsoring Agency Code

15. Supplementary Notes

16. Abstract

The cavitating and noncavitating performance of an 80.6° helical inducer with blunt blade leading edges (radius equal to one-half of blade thickness) was evaluated in liquid hydrogen. The inducer was operated at 30 000 rpm over a range of flow coefficients from 0.083 to 0.114 at liquid temperatures ranging from 31.2° to 39° R (17.3 to 21.7 K). The thermodynamic effect of cavitation increased with increasing temperature and ranged to 365 ft (112 m) at 39° R (21.7 K). The thermodynamic effect of cavitation also increased slightly with decreasing flow coefficient. Good agreement between experimental and predicted values of net positive suction head NPSH was obtained over the range of flow coefficient and temperature studied.

17. Key Words (Suggested by Author(s))	18. Distribution Statement
Hydrogen Cavitation Inducers	Unclassified - unlimited

19. Security Classif. (of this report)	20. Security Classif. (of this page)	21. No. of Pages	22. Price*
Unclassified	Unclassified	18	$3.00

*For sale by the Clearinghouse for Federal Scientific and Technical Information
Springfield, Virginia 22151

HYDROGEN CAVITATION PERFORMANCE OF 80.6° HELICAL INDUCER WITH BLUNT LEADING EDGES

by Phillip R. Meng and Royce D. Moore

Lewis Research Center

SUMMARY

The cavitating and noncavitating performance of an 80.6° helical inducer with blunt leading edge fairing (radius equal to one-half of blade thickness) was determined in liquid hydrogen. The net positive suction head requirements were determined over a range of liquid temperatures and flow coefficients at an inducer rotative speed of 30 000 rpm. Hydrogen temperatures ranged from 31.2° to 39° R (17.3 to 21.7 K) and flow coefficients from 0.083 to 0.114.

The thermodynamic effects of cavitation increased substantially with increasing liquid temperature and decreased with increasing flow coefficient. An available semi-empirical prediction method was used to predict the required net positive suction head NPSH for a given level of inducer performance. Good agreement was obtained between predicted and experimentally determined values of required net positive suction head.

INTRODUCTION

The inducer in a rocket engine turbopump is designed to operate satisfactorily with cavitation present on the suction surface of the blades. The evaporative cooling involved in the cavitation process causes the vapor pressure of the liquid surrounding a cavity to be reduced by an amount corresponding to the temperature reduction. The pressure within the cavity is reduced by a corresponding amount. This reduction in cavity pressure is equal to the change in the net positive suction head NPSH requirement for the inducer (refs. 1 to 4), where net positive suction head is defined as total pressure head above fluid vapor pressure head at the inducer inlet. Because of the evaporative cooling, the NPSH requirement of the inducer is less than it would be if the cooling did not occur. The amount of cooling realized is a function of the liquid, its temperature, the rotative speed and flow rate at which the inducer is operated, and also the geometric design of

the inducer.

The combined effects of fluid properties, flow conditions, and heat transfer are termed the thermodynamic effects of cavitation and, as shown in references 2 to 4, can improve the cavitation performance of inducers. The results from Venturi investigations (ref. 5) indicate that the geometric design of the inducer can affect the magnitude of the thermodynamic effects of cavitation because the size and shape of the cavity varies with the pressure distribution on the blade. The pressure distribution on an inducer blade is affected by the leading edge fairing and the fluid incidence angle. In previous tests of an 80.6° inducer (refs. 6 to 8), the blade leading edges were faired to a sharp wedge shape on the suction surface. However, in some cases the hydrodynamic loading over a range of operating conditions may result in blade material stress levels that could distort the thin leading edges. Therefore, for this investigation the blade leading edges were blunted to a radius equal to one-half of the blade thickness. The other geometric dimensions and the test ranges for flow and temperature were the same as in previous tests for the rotor so that the incidence angle would be unchanged.

The objective of this investigation was to determine the net positive suction head requirements for the 80.6° helical inducer with blunted blade leading edges. The inducer was operated in liquid hydrogen over a range of liquid temperature and flow coefficient. The results obtained were used in conjunction with a semiempirical prediction method (ref. 9) to predict the required net positive suction head and the magnitude of the thermodynamic effect of cavitation at various flow coefficients for several hydrogen temperatures. All tests were conducted at an inducer rotative speed of 30 000 rpm. Liquid temperatures ranged from 31.2° to 39° R (17.3 to 21.7 K) and flow coefficients from 0.083 to 0.114. The investigation was conducted at the Plum Brook Station of the NASA Lewis Research Center.

SYMBOLS

C_l	specific heat of liquid, Btu/(lbm)($^{\circ}$R); J/(kg)(K)
dh_v/dT	slope of curve of vapor pressure head against temperature, ft/$^{\circ}$R; m/K
g	acceleration due to gravity, ft/sec^2; m/sec^2
ΔH	pump head rise based on inlet density, ft of liquid; m of liquid
Δh_v	decrease in vapor pressure because of vaporization (magnitude of thermodynamic effect of cavitation), ft of liquid; m of liquid
k	liquid thermal conductivity, Btu/(hr)(ft)($^{\circ}$R); J/(hr)(m)(K)
L	latent heat of vaporization, Btu/lbm; J/kg
N	rotative speed, rpm

NPSH	net positive suction head, ft of liquid; m of liquid
U_t	blade tip speed, ft/sec; m/sec
V_a	average axial velocity at inducer inlet, ft/sec; m/sec
$\forall_l$	volume of liquid involved in cavitation process, $in.^3$; cm^3
$\forall_v$	volume of vapor, $in.^3$; cm^3
α	thermal diffusivity of liquid, $k/\rho_l C_l$, ft^2/hr; m^2/hr
ρ_l	density of liquid, lbm/ft^3; kg/cm^3
ρ_v	density of vapor, lbm/ft^3; kg/cm^3
φ	flow coefficient, V_a/U_t
ψ	head-rise coefficient, $g\,\Delta H/U_t^2$

Subscripts:

NC	noncavitating
ref	reference value obtained from experimental tests

APPARATUS AND PROCEDURE

Test Rotor

The test rotor used in this investigation was a three-bladed flat-plate helical inducer with a tip helix angle of 80.6°. The inducer was identical to that reported in references 6 to 8 except for the leading edge fairing. The leading edges of the inducer reported herein were rounded to a radius equal to one-half of the blade thickness, which resulted in a blunted leading edge. The radius of the leading edge varied from 0.075 inch (0.191 cm) at the hub to 0.050 inch (0.127 cm) at the tip because of the tapered blade thickness. A photograph and geometric details of the inducer are presented in figure 1.

Test Facility

This investigation was conducted in the liquid hydrogen pump test facility shown schematically in figure 2. The inducer was installed in an inlet annulus that extends 26.5 inches (67.3 cm) above the blade leading edges. The inducer was located near the bottom of the 2500-gallon ($9.5\text{-}m^3$) vacuum-jacketed research tank. A booster rotor located downstream of the inducer was used to overcome system losses. The flow path

C-69-1670

Tip helix angle (from axial direction), deg	80.6
Rotor tip diameter, in. (cm)	4.980 (12.649)
Rotor hub diameter, in. (cm)	2.478 (6.294)
Hub-tip ratio	0.496
Number of blades	3
Axial length, in. (cm)	2.00 (5.08)
Peripheral extent of blades, deg	280
Tip chord length, in. (cm)	12.35 (31.37)
Hub chord length, in. (cm)	6.36 (16.15)
Solidity at tip	2.350
Tip blade thickness, in. (cm)	0.100 (0.254)
Hub blade thickness, in. (cm)	0.150 (0.381)
Calculated radial tip clearance at hydrogen temperature, in. (cm)	0.025 (0.064)
Ratio of tip clearance to blade height	0.020
Material	6061-T6 Aluminum

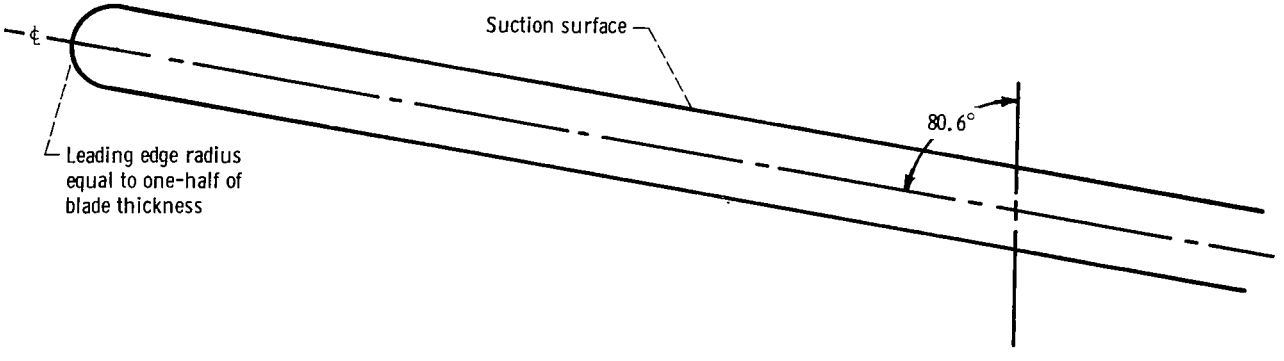

Figure 1. - Geometric details of 80.6° blunt leading edge inducer.

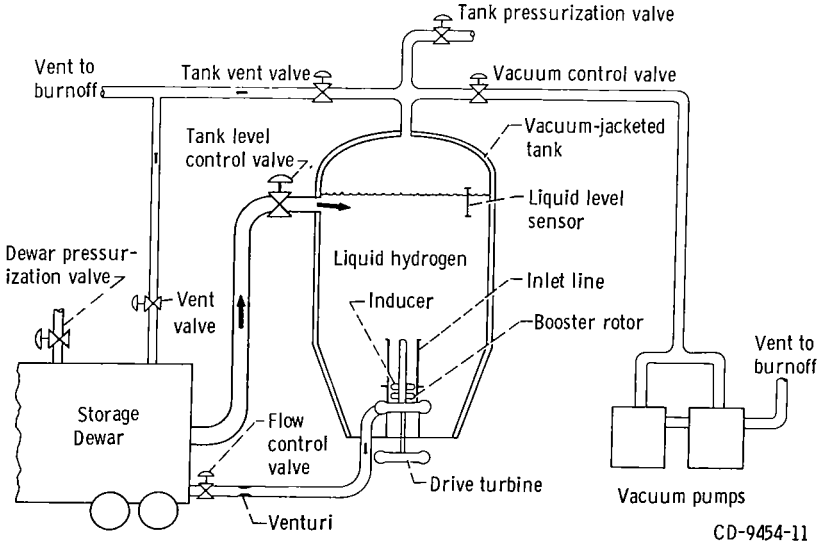

Figure 2. - Liquid hydrogen pump test facility.

is down the inlet annulus, through the inducer and booster rotor to a collector scroll, and into a discharge line to the storage Dewar.

The facility is basically the same as that described in references 2 and 4. For the tests reported herein, the same inlet line configuration used for the tests reported in reference 8 was used. The stationary centerbody extends from the entrance to the inlet line to the inducer hub and is held in place by four vanes at the entrance and three centering rods at the inducer end. The annulus formed by the inlet line and the centerbody has the same cross-sectional area as the inducer inlet area.

Test Procedure

The research tank was filled with liquid hydrogen from the storage Dewar. Prior to each test, the hydrogen in the tank was conditioned to the desired liquid temperature by vacuum for runs below 36.5° R (20.3 K) and by recirculation of the liquid for the higher temperature runs. The tank was then pressurized to 15 psi (10.4 N/cm^2) above the liquid vapor pressure. When the desired rotative speed was attained, the tank pressure (NPSH) was slowly reduced until the head rise deteriorated because of cavitation. The flow rate and bulk liquid temperature were maintained essentially constant during each test. The noncavitating performance was obtained by varying the flow rate while maintaining a constant rotative speed and liquid temperature. The tank pressure for the noncavitating runs was maintained at 15 psi (10.4 N/cm^2) above the liquid vapor pressure.

Instrumentation

The location of the instrumentation used in this investigation is shown schematically in figure 3. The measured parameters and the estimated maximum system errors are also listed in this figure.

The liquid vapor pressure was measured with two vapor pressure bulbs that were charged with hydrogen from the tank. One vapor pressure bulb was located at the entrance to the inlet line and the other at the inducer inlet. Tank pressure, measured in the ullage space, was used as the reference pressure for the differential pressure transducers. The liquid level above the inducer, measured by a capacitance gage, was added to the reference pressure to correct the differential pressures to the inducer inlet conditions. An averaged hydrogen temperature at the inducer inlet was obtained from two platinum resistor thermometers. A shielded total-pressure probe located at midpassage approximately 1 inch (2.54 cm) downstream of the test rotor was used to measure the inducer pressure rise. Pump flow rate was obtained with a Venturi flowmeter that was calibrated in water.

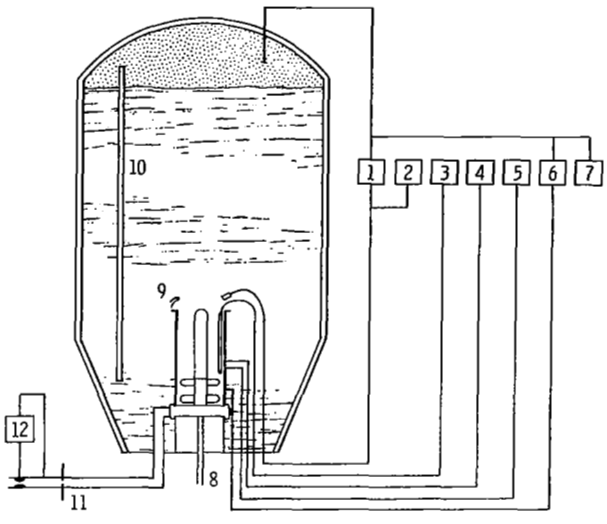

Item number	Parameter	Estimated system accuracy	Number of instruments used	Remarks
1	Tank net positive suction head, psi (N/cm^2)	Low range ±0.05 (±0.035)	1	Measured as differential pressure (converted to head of liquid) between vapor bulb at line inlet and tank pressure corrected to line inlet conditions
		High range ±0.25 (±0.17)	1	
2	Vapor pressure at line inlet, psi (N/cm^2)	±0.25 (±0.17)	1	Vapor bulb charged with liquid hydrogen from research tank
3	Vapor pressure at inducer inlet, psi (N/cm^2)	±0.25 (±0.17)	1	Long, small-diameter vapor bulb with streamlined trailing edge alined with flow stream to minimize bulb cavitation
4	Static pressure (line), psi (N/cm^2)	±0.05 (±0.035)	1	Average of three pressure taps (120° apart) located 10.5 in. (26.6 cm) above inducer inlet
5	Total pressure (line), psi (N/cm^2)	±0.05 (±0.035)	1	Shielded total pressure probe located 0.065 in. (0.165 cm) in from wall and 10.5 in. (26.6 cm) upstream of inducer
6	Inducer pressure rise, psi (N/cm^2)	±1.0 (±0.69)	1	Shielded total pressure probe at mid-passage 1 in. (2.54 cm) downstream of inducer
7	Tank pressure, psi (N/cm^2)	±0.5 (±0.35)	1	Measured in tank ullage and corrected to inducer inlet conditions for reference pressure for differential transducers
8	Rotative speed, rpm	±150	1	Magnetic pickup in conjunction with gear on turbine drive shaft
9	Line inlet temperature, °R (K)	±0.1 (±0.06)	2	Platinum resistor probes 180° apart at inlet
10	Liquid level, ft (m)	±0.5 (±0.15)	1	Capacitance gage, used for hydrostatic head correction to inducer inlet conditions
11	Venturi inlet temperature, °R (K)	±0.1 (±0.06)	1	Platinum resistor probe upstream of Venturi
12	Venturi differential pressure, psi (N/cm^2)	±0.25 (±0.17)	1	Venturi calibrated in air

Figure 3. - Instrumentation for liquid-hydrogen pump test facility.

The differential pressure measured directly between tank pressure and the vapor bulb at the annulus inlet was converted to feet of head (m of head) to obtain tank NPSH. Inducer NPSH was obtained by subtracting the annulus losses from the tank NPSH. The losses were calculated by multiplying the annulus fluid velocity head by the loss coefficient, which was determined to be 0.2 from calibrations in air.

RESULTS AND DISCUSSION

Noncavitating Performance

The noncavitating inducer performance is defined as that which shows no measurable decrease in inducer head rise when the NPSH is either increased or decreased. The noncavitating head-rise coefficient ψ_{NC} for the 80.6° inducer is plotted as a function of flow coefficient for an NPSH of 500 feet (153 m) in figure 4. The head-rise coefficient decreased almost linearly with increasing flow coefficient.

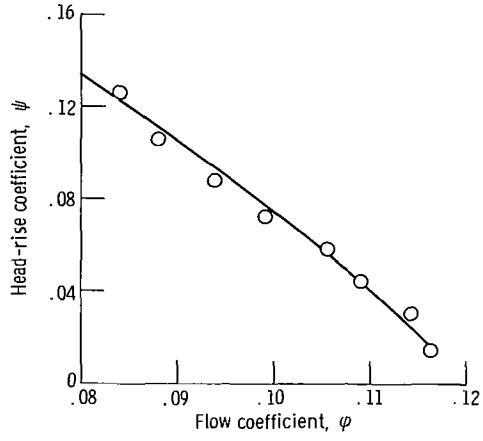

Figure 4. - Noncavitating performance of 80.6° blunt-leading-edge inducer in hydrogen at 30 000 rpm. Nominal hydrogen temperature, 36.6° R (20.3 K).

Cavitating Performance

The cavitating performance for the 80.6° helical inducer with blunted leading edges is shown in figure 5. The inducer head-rise coefficient is shown as a function of the NPSH at the inducer inlet for a range of flow coefficients at each of several hydrogen inlet temperatures. The data of figure 5 show that, for a given performance level, the required NPSH increases with increasing flow coefficient at each liquid temperature.

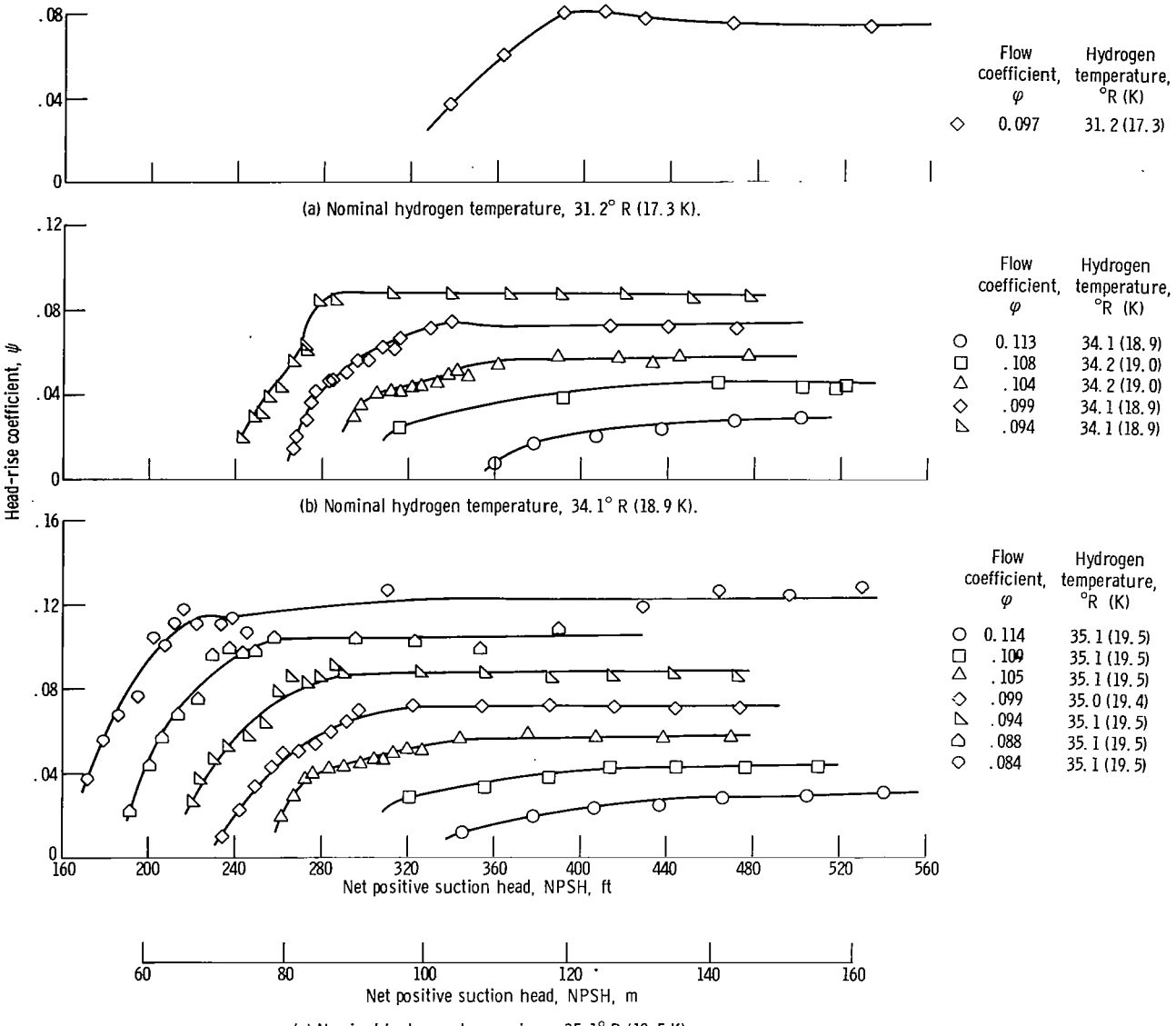

Figure 5. - Cavitating performance of 80.6° blunt-leading-edge inducer in hydrogen at 30 000 rpm.

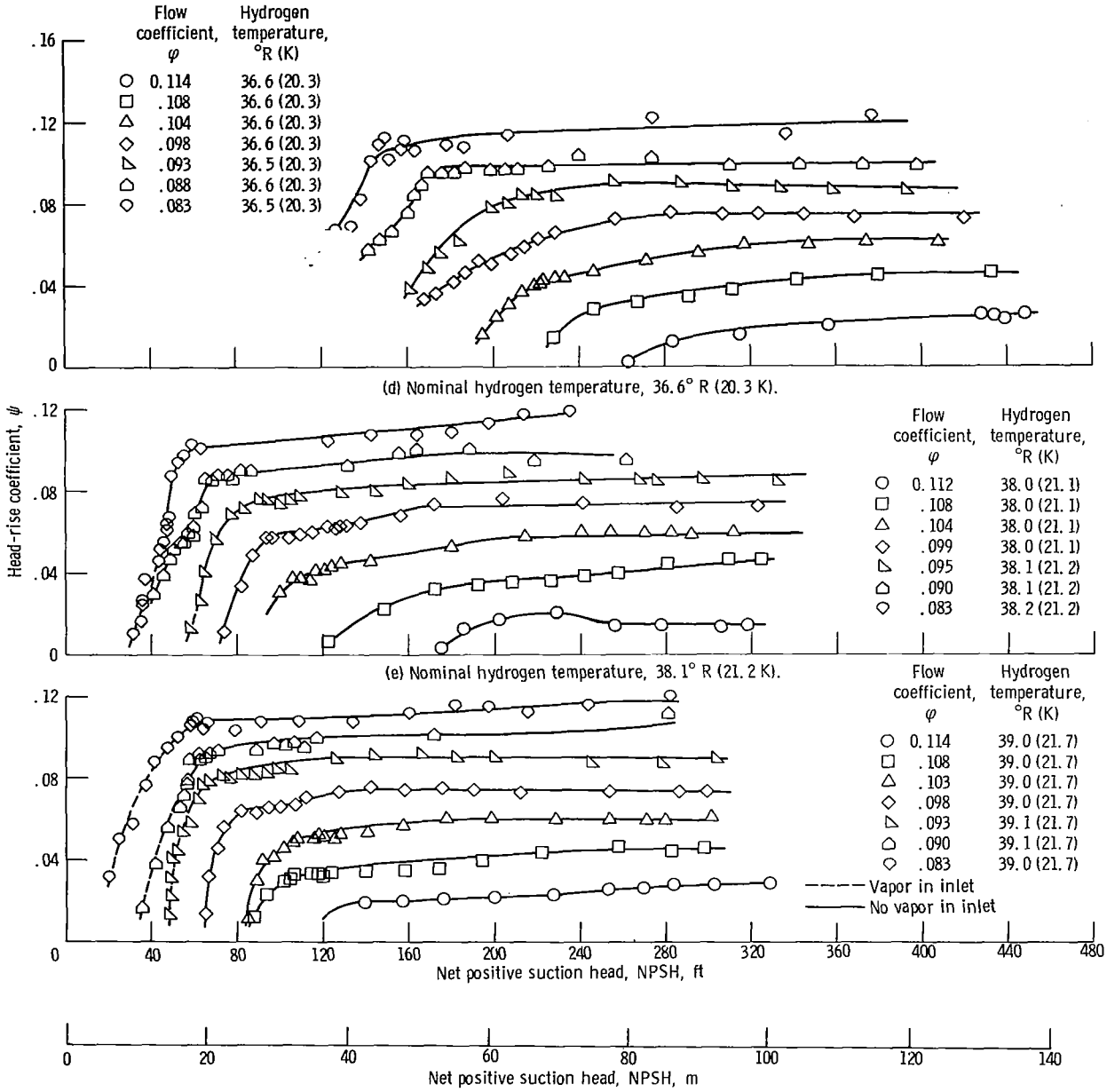

(f) Nominal hydrogen temperature, 39.0° R (21.7 K).

Figure 5. - Concluded.

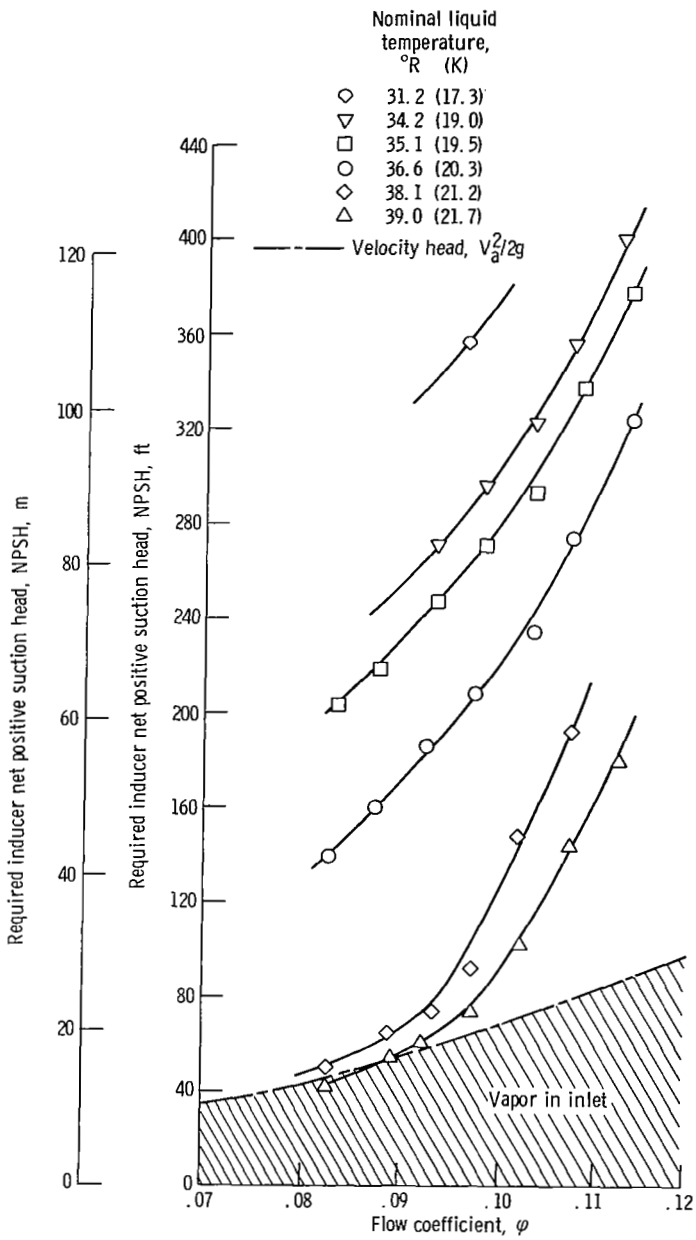

Figure 6. - Variation of inducer cavitation performance with flow coefficient at several hydrogen temperatures. Rotative speed, 30 000 rpm; head-rise-coefficient ratio, 0.70.

These data also show that a higher NPSH is required for a given performance level as the temperature of the hydrogen is lowered. The data for a liquid temperature of 31.2° R (17.3 K) shown in figure 5(a) are for only one value of flow coefficient. Because of operational difficulties at the lower hydrogen temperatures, data were not taken at all values of flow coefficient at the 31.2° and 34.1° R (17.3 and 18.9 K) hydrogen temperatures.

The required inducer NPSH for a head-rise-coefficient ratio ψ/ψ_{NC} of 0.70 is shown in figure 6 as a function of flow coefficient for a range of liquid temperatures. The shaded area in the figure represents the values of NPSH that are below the fluid velocity head $V_a^2/2g$ at the inducer inlet. When the NPSH is lowered to the value of the inlet velocity head, the local static pressure in the inlet becomes equal to the fluid vapor pressure. As the pressure is further reduced, the fluid begins to boil in the inlet, and vapor is ingested by the inducer. Vapor ingestion causes an increase in the through-flow velocity and a subsequent shift to a higher flow coefficient (ref. 10).

Thermodynamic Effects of Cavitation

A method for predicting the thermodynamic effects of cavitation and the cavitation performance of inducers is presented in detail in reference 9. A brief resume of this method is presented herein. A heat balance between the heat required for vaporization and that drawn from the liquid adjacent to the cavity is used to estimate the cavity pressure depression below free-stream vapor pressure:

$$\Delta h_v = \left(\frac{\rho_v}{\rho_l}\right)\left(\frac{L}{C_l}\right)\left(\frac{dh_v}{dT}\right)\left(\frac{\gamma_v}{\gamma_l}\right) \tag{1}$$

With the properties of hydrogen known, values of vapor- to liquid-volume ratio γ_v/γ_l as a function of Δh_v can be obtained by numerical integration of equation (1). This takes into account changes in properties as the equilibrium temperature drops because of the evaporative cooling. The calculated depression in vapor pressure Δh_v is plotted as a function of vapor- to liquid-volume ratio γ_v/γ_l for a range of liquid hydrogen temperatures in figure 7. Equation (1) cannot be used directly to predict the required NPSH because the absolute value of γ_v/γ_l is not known. However, it has been shown that, if a reference value of γ_v/γ_l is established experimentally by determining Δh_v, values of γ_v/γ_l relative to this reference value can be estimated from the following equation:

$$\frac{\gamma_v}{\gamma_l} = \left(\frac{\gamma_v}{\gamma_l}\right)_{ref}\left(\frac{\alpha_{ref}}{\alpha}\right)\left(\frac{N}{N_{ref}}\right)^{0.8} \tag{2}$$

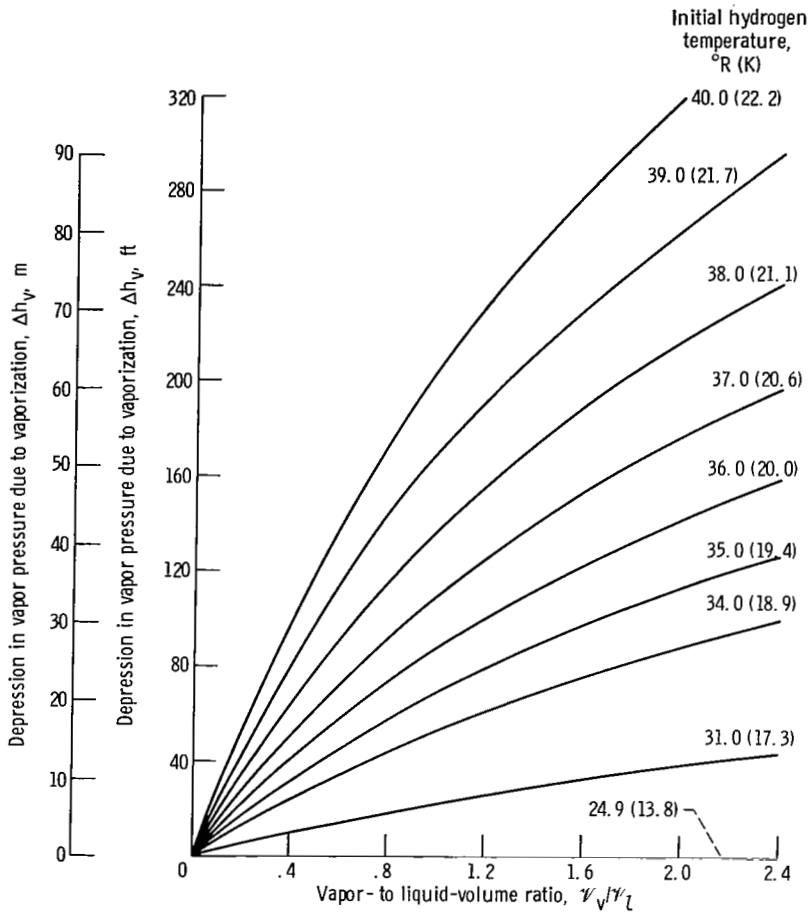

Figure 7. - Calculated vapor pressure depression due to vaporization as function of volume ratio for several liquid hydrogen temperatures.

Equation (2) assumes geometrically similar cavitating flow conditions (i.e., the same flow coefficient and the same head-rise-coefficient ratio for the predicted condition as those for the reference condition).

The inducer cavitation performance for a constant flow coefficient and head-rise-coefficient ratio is predicted by use of the following equation from reference 9:

$$\frac{NPSH + \Delta h_v}{NPSH_{ref} + (\Delta h_v)_{ref}} = \left(\frac{N}{N_{ref}}\right)^2 \tag{3}$$

This relation requires that two experimental test points be available for the inducer of interest. These experimental data can be for any combination of liquid, liquid temperature, or rotative speed, provided that at least one set of data exhibits a measurable thermodynamic effect. From these experimental data, the cavitation performance for

the inducer can be predicted for any liquid, liquid temperature, or rotative speed. For the present study, only changes in liquid temperature at specified flow coefficients are considered.

The 35.1° and 36.6° R (19.5 and 20.3 K) temperature curves of figure 6 were used as reference values with the semiempirical relation of reference 9 to predict the thermodynamic effect of cavitation over the range of flow coefficient. The predicted magnitude of the thermodynamic effect of cavitation is shown in figure 8 as a function of flow coefficient for a range of liquid hydrogen temperatures. The liquid temperatures were chosen to coincide with the nominal test temperatures of the data presented in figure 6. Since the thermodynamic effect of cavitation is zero at the triple-point temperature of 24.9° R

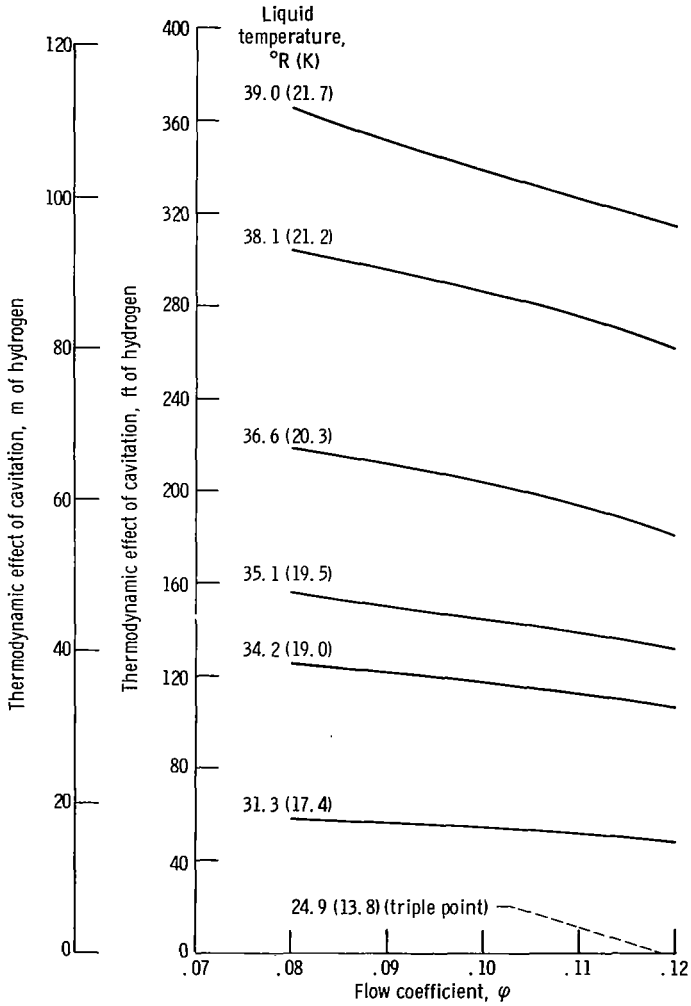

Figure 8. - Predicted thermodynamic effects of cavitation as function of flow coefficient at several hydrogen temperatures for an 80.6° blunt-leading-edge inducer. Rotative speed, 30 000 rpm; head-rise-coefficient ratio, 0.70.

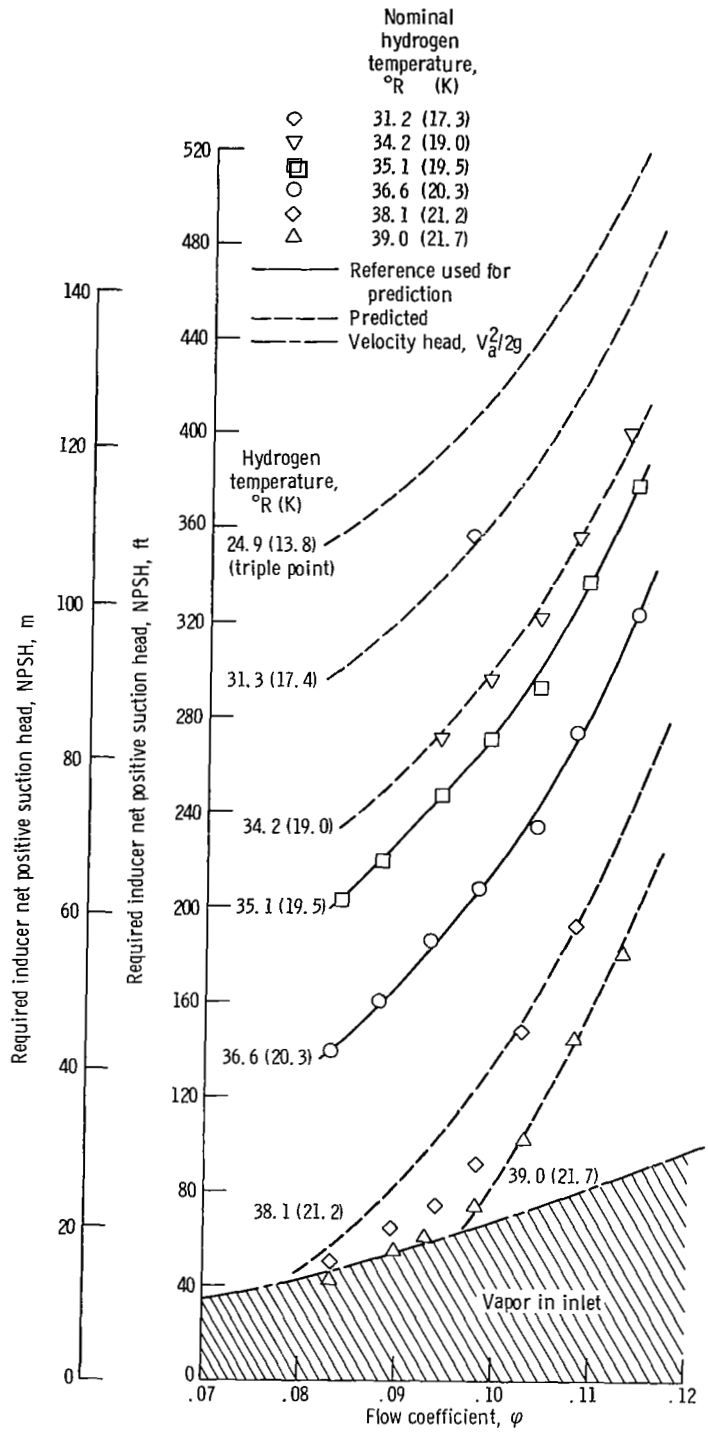

Figure 9. - Comparison of predicted and measured net positive suction head for 80.6° blunt-leading-edge inducer in hydrogen. Rotative speed, 30 000 rpm; head-rise-coefficient ratio, 0.70.

(13.8 K), the predicted curve for the triple point is the abscissa of figure 8. The trend of increasing thermodynamic effect of cavitation with temperature noted in figure 8 was also observed for this inducer with a faired leading edge (ref. 11), but the magnitude of the thermodynamic effect of cavitation is considerably greater for the inducer with the blunt leading edge. This trend was observed at all values of flow coefficient for each of the liquid temperatures. For example, at a liquid temperature of 36.6° R (20.3 K) and a flow coefficient of 0.10, the magnitude of the thermodynamic effect for the inducer with the blunt leading edge is 203 feet (62 m) as compared with 168 feet (51 m) for the same inducer with a faired leading edge. Although the thermodynamic effect of cavitation is greater, the required NPSH at a given temperature is significantly greater for the blunt-leading-edge inducer than for the faired-leading-edge inducer of reference 11. The difference in the magnitude of the thermodynamic effect of cavitation is attributed to the variation in the blade pressure distribution resulting from the two different leading edge fairings (ref. 5). The curves in figure 8 also show that the thermodynamic effect of cavitation increases slightly as the flow coefficient is decreased. For this effect, the change in blade pressure distribution is attributed to the change in incidence angle. This trend of the thermodynamic effect varying with flow coefficient was also noted for an 84° helical inducer in reference 4.

A comparison between the experimental and predicted values of required inducer NPSH for the inducer at a head-rise-coefficient ratio of 0.70 is shown in figure 9. The data points are repeated from figure 6, and the reference data at 35.1° and 36.6° R (19.5 and 20.3 K), which were used to predict the required NPSH at the other temperatures, are indicated by solid lines. The predicted values are shown as dashed lines. The liquid hydrogen data at 31.3° and 34.2° R (17.4 and 19.0 K) compare very well with the predicted curves. The hydrogen data at 39.0° R (21.7 K) compare fairly well with the predicted curves for those values of NPSH greater than the calculated velocity head $V_a^2/2g$. The values of NPSH below the calculated velocity head $V_a^2/2g$ are again indicated by the shaded area. The data at 38.1° R (21.2 K) compare well with the predicted curve at the higher values of flow coefficient, but some disagreement occurs at the lower values of flow coefficient where the NPSH approaches the calculated velocity head.

SUMMARY OF RESULTS

The net positive suction head NPSH requirements for an 80.6° helical inducer with a blunted blade leading edge fairing were evaluated in hydrogen over a liquid temperature range from 31.2° to 39° R (17.3 to 21.7 K). The inducer was tested over a range of flow coefficients from 0.083 to 0.114 at a rotative speed of 30 000 rpm.

The thermodynamic effects of cavitation were predicted over the range of hydrogen

temperatures and flow coefficient using an available semiempirical method. A comparison between the experimental and predicted values of required net positive suction head was made. This investigation yielded the following principal results:

1. The predicted magnitude of the thermodynamic effect of cavitation increased substantially with increasing liquid temperature and decreased with increasing flow coefficient. The thermodynamic effects of cavitation ranged to 365 feet (112 m) at a liquid temperature of 39.0° R (21.7 K).

2. In general, good agreement was obtained between the predicted and experimentally determined values of NPSH over the range of flow coefficient and liquid hydrogen temperature studied.

3. Higher values of NPSH were required to maintain a given inducer performance level, because of a decrease in the magnitude of the thermodynamic effect, as the hydrogen inlet temperature was lowered.

Lewis Research Center,
National Aeronautics and Space Administration,
Cleveland, Ohio, May 8, 1970,
128-31.

REFERENCES

1. Gelder, Thomas F.; Ruggeri, Robert S.; and Moore, Royce D.: Cavitation Similarity Considerations Based on Measured Pressure and Temperature Depressions in Cavitated Regions of Freon-114. NASA TN D-3509, 1966.

2. Ball, Calvin L.; Meng, Phillip R.; and Reid, Lonnie: Cavitation Performance of 84° Helical Pump Inducer Operated in 37° and 42° R Liquid Hydrogen. NASA TM X-1360, 1967.

3. Ruggeri, Robert S.; Moore, Royce D.; and Gelder, Thomas F.: Method for Predicting Pump Cavitation Performance. Paper presented at the ICRPG Ninth Liquid Propulsion Symposium, St. Louis, Oct. 25-27, 1967.

4. Meng, Phillip R.: Change in Inducer Net Positive Suction Head Requirement with Flow Coefficient in Low Temperature Hydrogen (27.9° to 36.6° R). NASA TN D-4423, 1968.

5. Moore, Royce D.; Ruggeri, Robert S.; and Gelder, Thomas F.: Effects of Wall Pressure Distribution and Liquid Temperature on Incipient Cavitation of Freon-114 and Water in Venturi Flow. NASA TN D-4340, 1968.

6. Meng, Phillip R.; and Moore, Royce D.: Cavitation Performance of 80.6° Helical Inducer in Liquid Hydrogen. NASA TM X-1808, 1969.

7. Moore, Royce D.; and Meng, Phillip R.: Cavitation Performance of Line-Mounted 80.6° Helical Inducer in Hydrogen. NASA TM X-1854, 1969.

8. Meng, Phillip R.; and Moore, Royce D.: Hydrogen Cavitation Performance of 80.6° Helical Inducer Mounted in Line with Stationary Centerbody. NASA TM X-1935, 1970.

9. Ruggeri, Robert S.; and Moore, Royce D.: Method for Prediction of Pump Cavitation Performance for Various Liquids, Liquid Temperatures, and Rotative Speeds. NASA TN D-5292, 1969.

10. Meng, Phillip R.; and Connelly, Robert E.: Investigation of Effects of Simulated Nuclear Radiation Heating on Inducer Performance in Liquid Hydrogen. NASA TM X-1359, 1967.

11. Moore, Royce D.; and Meng, Phillip R.: Thermodynamic Effects of Cavitation of an 80.6° Helical Inducer Operated in Hydrogen. NASA TN D-5614, 1970.

NASA-Langley, 1970 —— 12 E-5495

"The aeronautical and space activities of the United States shall be conducted so as to contribute . . . to the expansion of human knowledge of phenomena in the atmosphere and space. The Administration shall provide for the widest practicable and appropriate dissemination of information concerning its activities and the results thereof."

—NATIONAL AERONAUTICS AND SPACE ACT OF 1958

NASA SCIENTIFIC AND TECHNICAL PUBLICATIONS

TECHNICAL REPORTS: Scientific and technical information considered important, complete, and a lasting contribution to existing knowledge.

TECHNICAL NOTES: Information less broad in scope but nevertheless of importance as a contribution to existing knowledge.

TECHNICAL MEMORANDUMS: Information receiving limited distribution because of preliminary data, security classification, or other reasons.

CONTRACTOR REPORTS: Scientific and technical information generated under a NASA contract or grant and considered an important contribution to existing knowledge.

TECHNICAL TRANSLATIONS: Information published in a foreign language considered to merit NASA distribution in English.

SPECIAL PUBLICATIONS: Information derived from or of value to NASA activities. Publications include conference proceedings, monographs, data compilations, handbooks, sourcebooks, and special bibliographies.

TECHNOLOGY UTILIZATION PUBLICATIONS: Information on technology used by NASA that may be of particular interest in commercial and other non-aerospace applications. Publications include Tech Briefs, Technology Utilization Reports and Notes, and Technology Surveys.

Details on the availability of these publications may be obtained from:

SCIENTIFIC AND TECHNICAL INFORMATION DIVISION

NATIONAL AERONAUTICS AND SPACE ADMINISTRATION

Washington, D.C. 20546